Applied Physics Letters

Evidence for monoclinic crystal structure and negative thermal expansion below magnetic transition temperature in $Pb(Fe_{1/2}Nb_{1/2})O_3$

Cite as: Appl. Phys. Lett. **90**, 242915 (2007); https://doi.org/10.1063/1.2748856
Submitted: 07 April 2007 . Accepted: 22 May 2007 . Published Online: 14 June 2007

Satendra Pal Singh, Dhananjai Pandey, Songhak Yoon, Sunggi Baik, Namsoo Shin, et al.

View Online Export Citation

ARTICLES YOU MAY BE INTERESTED IN

Spin-lattice coupling in multiferroic Pb(Fe1/2Nb1/2)O3 thin films
Applied Physics Letters **94**, 012509 (2009); https://doi.org/10.1063/1.3067872

Frequency-temperature response of ferroelectromagnetic Pb(Fe1/2Nb1/2)O3 ceramics obtained by different precursors. Part I. Structural and thermo-electrical characterization
Journal of Applied Physics **97**, 084107 (2005); https://doi.org/10.1063/1.1870099

$BaTiO_3$-based piezoelectrics: Fundamentals, current status, and perspectives
Applied Physics Reviews **4**, 041305 (2017); https://doi.org/10.1063/1.4990046

Challenge us.
What are your needs for periodic signal detection?
Watch

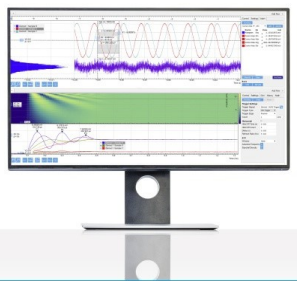

Zurich Instruments

AIP Publishing

© 2007 American Institute of Physics.

Evidence for monoclinic crystal structure and negative thermal expansion below magnetic transition temperature in $Pb(Fe_{1/2}Nb_{1/2})O_3$

Satendra Pal Singh and Dhananjai Pandey[a)]
School of Materials Science and Technology, Institute of Technology, Banaras Hindu University, Varanasi-221 005, India

Songhak Yoon and Sunggi Baik
Department of Materials Science and Engineering, Pohang University of Science and Technology, Pohang 790-784, Korea

Namsoo Shin
Pohang Accelerator Laboratory, Pohang University of Science and Technology, Pohang 790-784, Korea

(Received 7 April 2007; accepted 22 May 2007; published online 14 June 2007)

The existing controversy about the room temperature structure of multiferroic $Pb(Fe_{1/2}Nb_{1/2})O_3$ is settled using synchrotron powder x-ray diffraction data. Results of Rietveld refinements in the temperature range of 300–12 K reveal that the structure remains monoclinic in the *Cm* space group down to 12 K, but the lattice parameters show anomalies at the magnetic transition temperature (T_N) due to spin-lattice coupling. The lattice volume exhibits negative thermal expansion behavior, with $\alpha=-4.64\times10^{-6}K^{-1}$, below T_N. © *2007 American Institute of Physics*. [DOI: 10.1063/1.2748856]

Recent years have witnessed enormous interest in multiferroic materials due to their potential applications in memory, sensor, and actuator devices.[1] Lead iron niobate, $Pb(Fe_{1/2}Nb_{1/2})O_3$ (PFN), is a multiferroic material exhibiting paraelectric to ferroelectric[2] and paramagnetic to *G*-type antiferromagnetic[3,4] transitions at 385 and 143 K, respectively. It is an attractive material for use in multilayer ceramic capacitors and other electronic devices due to its high dielectric constant (>10 000), diffuse phase transition behavior,[5] and low sintering temperature.[6] However, there exist controversies about the structure of PFN at room temperature until now. Both rhombohedral[7] and monoclinic[8,9] structures in the *R*3*m* and *Cm* space groups, respectively, have been proposed, but more careful investigation is still needed to obtain a clear picture about the correct crystal structure of PFN.

In a recent temperature dependent dielectric study, a jump in the dielectric constant near the Néel temperature $T_N=143$ K has been reported.[4] Using earlier Landau theory results,[10] Yang *et al.* have shown that the change in the dielectric constant at Néel temperature may be associated with the magnetoelectric coupling term γP^2M^2, where *P*, *M*, and γ are polarization, magnetization, and magnetoelectric coupling coefficient, respectively. A similar change in the dielectric constant at Néel temperature has been reported in other magnetoelectric materials such as RMn_2O_5 and $RMnO_3$ (*R*=Tb, Ho, and Dy).[1,10–13] In the RMn_2O_5 family of magnetoelectrics, changes in the cell parameters at the Néel temperature have also been reported and it has been interpreted as a signature of spin-lattice coupling in such magnetoelectrics.[12,13] No attempt has been made so far to look for the anomalies in the unit cell parameters as a result of magnetoelectric coupling in PFN.

In this letter, we present the results of Rietveld analysis of high resolution synchrotron x-ray diffraction (XRD) data to resolve the existing controversies about the structure of PFN at room temperature. After settling the room temperature structure of PFN, we have also carried out Rietveld analysis of powder XRD data, collected at different temperatures in the range of 300–12 K, to see if there is any lattice parameter anomaly associated with the magnetic transition. It is shown that the structure of PFN is monoclinic in the *Cm* space group in the entire temperature range of 300–12 K of our study. It is also shown that the lattice parameters and unit cell volume show distinct anomaly at T_N, with unambiguous evidence of negative thermal expansion below T_N.

Pyrochlore free PFN samples were prepared by solid-state route, the details of which are described elsewhere.[14] For x-ray characterization, the sintered pellets were crushed to fine powders and then annealed at 500 °C for 10 h to remove the strains introduced during crushing. XRD measurements were carried out using an 18 kW rotating anode (Cu $K\alpha$) based Rigaku powder diffractometer operating in the Bragg-Brentano geometry and fitted with a graphite monochromator in the diffracted beam and attached with a close cycle He-refrigerator for varying the sample temperature continuously in the temperature range of 300–12 K. The data weere collected in the 2θ range of 20°–120° at a step length of 0.02° during heating after cooling the sample to 12 K. Synchrotron powder XRD experiments were carried out at 8C2 HRPD beamline at Pohang Light Source (PLS). The incident x-rays were monochromatized to the wavelength of 1.543 Å by a double bounce Si (111) monochromator. The diffraction pattern was scanned in the 2θ range of 20°–130° at a step length of 0.01°. Rietveld refinements were carried out using FULLPROF program.[15] In the refinements, pseudo-Voigt function and a fifth order polynomial were used to define the profile shape and the background, respectively. Except for the occupancy parameters of the ions, which were fixed at the nominal composition, all other parameters, such as scale factor, zero correction, background, half-width parameters, the mixing parameters, lattice parameters, positional coordinates, and thermal parameters, were varied in the course of refinement. It was found necessary to

[a)]Author to whom correspondence should be addressed; electronic mail: dpandey@bhu.ac.in

 © 2007 American Institute of Physics

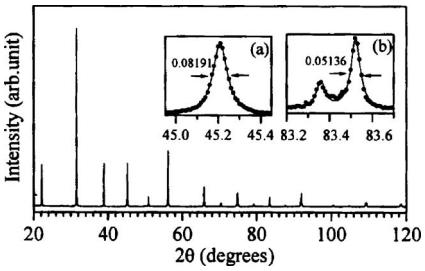

FIG. 1. Synchrotron x-ray powder diffraction pattern of $Pb(Fe_{1/2}Nb_{1/2})O_3$ at room temperature. Insets (a) and (b) show the zoomed profiles of the pseudocubic 200 and 222 reflections, respectively.

use anisotropic peak broadening for the synchrotron data, whereas the laboratory data could be analyzed using isotropic peak broadening function only. The isotropic thermal parameter for Pb was found to be considerably large (~2.216) indicating Pb-site disorder, as reported by earlier workers[9] and the use of anisotropic thermal parameters in the refinements resulted in lower χ^2 values. For the rhombohedral phase with $R3m$ space group, we have used hexagonal axes with lattice parameters $a_H=b_H=\sqrt{2}a_R$ and $c_H=\sqrt{3}a_R$, where a_R corresponds to the rhombohedral cell parameter.

Synthesis of phase pure perovskite PFN is a major challenge, as the pyrochlore phases such as $Pb_2Nb_2O_7$ and $Pb_2Nb_4O_{13}$ get easily formed.[16] Using a modified solid state route,[14] we were able to synthesize pyrochlore free PFN samples. Figure 1 depicts the synchrotron powder XRD pattern of PFN at room temperature. There are no peaks near $2\theta \approx 28.84°$ or 29.25°, which are the strongest XRD peaks for the $Pb_2Nb_2O_7$ and $Pb_2Nb_4O_{13}$, confirming the absence of the pyrochlore phase. All the peaks in this figure correspond to the perovskite PFN phase. The inset depicts the zoomed profiles of the pseudocubic 200 and 222 reflections which are singlet and doublet, respectively, indicating a rhombohedral structure at first sight. However, if 200 peak is truly singlet, as expected for the rhombohedral structure, its width should have been less than that of the pseudocubic 222 peak following Caglioti relationship for the 2θ dependence of the peak width.[17] The width of 200 peak is about 1.6 times that of the 222 pseudocubic peak and it suggests that 200 peak is not singlet, and hence the true structure may not be rhombohedral. A similar anomalous broadening of the 200 peak in $Pb(Zr_xTi_{1-x})O_3$ (PZT) and $(1-x)[Pb(Mg_{1/3}Nb_{2/3})O_3]$-$xPbTiO_3$ (PMN-xPT) has been attributed to a short range ordered monoclinic phase in the Cm space group.[18] A choice between the $R3m$ and Cm space groups in these materials was made unambiguously using profile refinement techniques.

Figure 2 presents the Rietveld fits for 200, 220, and 222 pseudocubic profiles obtained after full pattern refinements using rhombohedral and monoclinic structural models for PFN. For the rhombohedral model, if we try to account for the large broadening of the 200 reflection, the fit for the 222 reflection becomes very poor, as is evident from Fig. 2(a). On the other hand, if we try to force good fit for the 222 reflection, the fit for 200 and other reflections becomes poor, as shown in Fig. 2(b). Very good fit, however, is obtained for all the other reflections if one uses the monoclinic structure in the Cm space group, as shown in Fig. 2(c). The agreement factors, the Durbin-Watson statistics,[19] and Prince's criterion[14] favor the Cm space group. Table I lists the refined

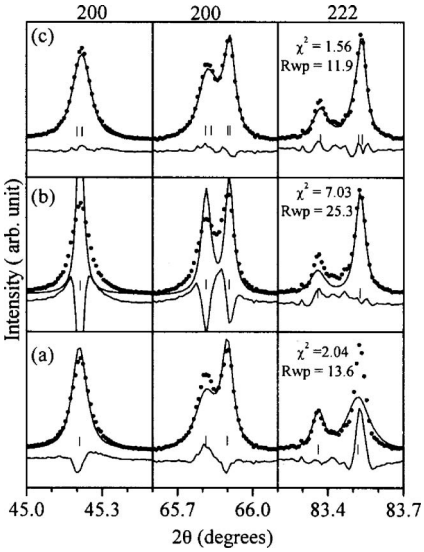

FIG. 2. Observed (dots), calculated (continuous line), and difference (bottom line) profiles of the 200, 220, and 222 pseudocubic reflections obtained after full pattern Rietveld refinements using the room temperature synchrotron powder diffraction data of $Pb(Fe_{1/2}Nb_{1/2})O_3$ in the 2θ range of 20°–130°: (a) and (b) rhombohedral $R3m$ space group and (c) monoclinic Cm space group. The tick marks above the difference plot show the position of the Bragg peaks.

structural parameters for the monoclinic Cm space group. The equivalent elementary perovskite cell parameters of the monoclinic Cm of PFN bear the relationship $a_m/\sqrt{2} \approx b_m/\sqrt{2} < c_m$, and hence this phase is of M_A type in the notation of Vanderbilt and Cohen.[20]

Having settled the room temperature structure of PFN unambiguously, we carried out Rietveld refinements with the monoclinic structure in the Cm space group for the low temperature XRD data in order to investigate the effect of magnetoelectric coupling on the structure of PFN near T_N. We find that the monoclinic structure remains unchanged below T_N. Figure 3 shows lattice parameters, unit cell volume, and the monoclinic distortion angle (β) of PFN as a function of temperature. All the three lattice parameters (a, b, and c) show anomalies around 150 K, which is close to the magnetic transition temperature reported in the literature.[21] The monoclinic distortion angle (β), however, does not show any anomaly and increases continuously as the temperature decreases. The lattice parameter b becomes nearly temperature independent below 150 K whereas lattice parameters a and c

TABLE I. Refined structural parameters of $Pb(Fe_{1/2}Nb_{1/2})O_3$ using monoclinic structure in the Cm space group.

a_m=5.6787(1) Å; b_m=5.673 10(9) Å; c_m=4.015 20(9) Å;
$\alpha=\gamma$=90.00° and β=90.098(7)°

Ions	x	y	z	B (Å^2)
Pb^{+2}	0.0000	0.0000	0.0000	β_{11}=0.015(2)
				β_{22}=0.022(2)
				β_{33}=0.029(4)
				β_{13}=0.008(1)
Fe^{+3}/Nb^{+5}	0.510(3)	0.0000	0.478(3)	B=0.23(7)
O^{-2}_{I}	0.53(1)	0.0000	–0.04(1)	B=0.6(3)
O^{-2}_{II}	0.273(8)	0.254(8)	0.44(1)	B=0.4(2)

R_p=8.69; R_{wp}=11.9; R_{expt}=9.53; χ^2=1.56

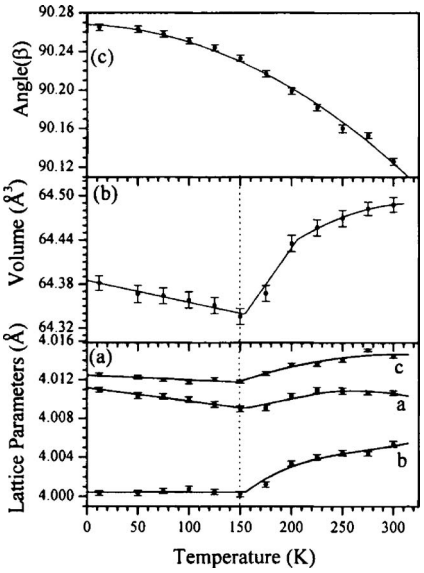

FIG. 3. Temperature dependent variation of (a) lattice parameters (a, b, and c), (b) unit cell volume, and (c) the monoclinic distortion angle (β) obtained from Rietveld refinements using powder x-ray diffraction data. The equivalent elementary perovskite cell parameters are calculated as $a=a_m/\sqrt{2}$, $b=a_m/\sqrt{2}$, and $c=c_m$.

exhibit negative thermal expansion. The volume of the unit cell first decreases on cooling up to 150 K and then starts to increase below 150 K, showing a negative volume thermal expansion at $T<T_N$. The linear negative thermal expansion coefficient (α) obtained from the fit in Fig. 3(b) at $T\leqslant 150$ K is -4.64×10^{-6} K^{-1}.

The observation of anomalies in the temperature dependence of dielectric constant[10,11] and ferroelectric polarization at magnetic transition temperatures are taken as evidence for magnetoelectric effect due to spin-lattice coupling.[11,22] Such a coupling is also expected to lead to anomalies in the lattice parameters. However, the earlier studies for resolving such lattice parameter anomalies using scattering techniques in materials such as $HoMn_2O_5$ and $DyMn_2O_5$ (Ref. 13) have failed to provide any evidence. Very weak anomalies at T_N have been reported in $TbMn_2O_5$.[12] In $DyMn_2O_5$; this anomaly is somewhat more pronounced and there is a sign of negative thermal expansion also below T_N.[13] In comparison, the lattice parameter and the unit cell volume anomalies are well pronounced in PFN. The existence of negative thermal expansion below T_N clearly suggests that the thermal contraction below T_N due to anharmonicity is being more than offset by the magnetic ordering. We believe that the ferromagnetic component of the G-type antiferromagnetic state below T_N is responsible for the negative thermal expansion due to the spin-lattice coupling. In $SrRuO_3$, there is also competition between the lattice and the magnetic contributions to the overall thermal expansion behavior below the magnetic transition temperature.[23] This has been attributed to a magnetovolume effect arising from itinerant electron magnetism. It remains to be seen whether this mechanism is responsible for the negative thermal expansion in PFN. We hope that our results will encourage some *ab initio* first principles calculations to understand the role of magnetic ordering on the thermal expansion behavior, which may in turn throw light on the magnetoelectric coupling.

One of the authors S. P. S. acknowledges financial support from the All India Council of Technical Education (AICTE) in the form of the award of a National Doctoral Fellowship (NDF). The experiments at Pohang Light Source (PLS) were supported by the Ministry of Science and Technology (MOST) and POSTECH, Pohang, Korea.

[1] N. Hur, S. Park, P. A. Sharma, J. S. Ahn, S. Guha, and S.-W. Cheong, Nature (London) **429**, 329 (2004); M. Fiebig, J. Phys. D **38**, R123 (2005); W. Eerenstein, N. D. Mathur, and J. F. Scott, Nature (London) **442**, 759 (2006).
[2] G. A. Smolenskii, A. I. Agranovskaia, S. N. Popov, and V. A. Isupov, Sov. Phys. Tech. Phys. **3**, 1981 (1958).
[3] V. A. Bokov, I. I. Mylnikova, and G. A. Smolenskii, Sov. Phys. JETP **15**, 447 (1962).
[4] Y. Yang, J. M. Liu, H. B. Huang, W. Q. Zou, P. Bao, and Z. G. Liu, Phys. Rev. B **70**, 132101 (2004).
[5] S. P. Singh, A. K. Singh, D. Pandey, H. Sharma, and O. Parkash, J. Mater. Res. **18**, 2677 (2003).
[6] M. Yonezawa, Am. Ceram. Soc. Bull. **62**, 1375 (1983).
[7] I. H. Brunskill, R. Boutellier, W. Depmeier, H. Schmid, and H. J. Sheel, J. Cryst. Growth **56**, 541 (1982); S. A. Mabud, Phase Transitions **4**, 183 (1984); S. A. Ivonov, R. Tellgren, H. Rundlof, N. W. Thomas, and S. Ananta, J. Phys.: Condens. Matter **12**, 2393 (2000).
[8] V. Bonny, M. Bonin, P. Sciau, K. J. Schenk, and G. Chapuis, Solid State Commun. **102**, 347 (1997).
[9] N. Lampis, P. Sciau, and A. G. Lehmann, J. Phys.: Condens. Matter **11**, 3489 (1999).
[10] T. Kimura, S. Kawamoto, I. Yamada, M. Azuma, M. Takano, and Y. Tokura, Phys. Rev. B **67**, 180401 (2003).
[11] T. Kimura, T. Goto, H. Shintani, K. Ishizaka, T. Arima, and Y. Tokura, Nature (London) **426**, 55 (2003)
[12] L. C. Chapon, G. R. Blake, M. J. Gutmann, S. Park, N. Hur, P. G. Radaelli, and S.-W. Cheong, Phys. Rev. Lett. **93**, 107207 (2004).
[13] G. R. Blake, L. C. Chapon, P. G. Radaelli, S. Park, N. Hur, S.-W. Cheong, and J. Rodríguez-Carvajal, Phys. Rev. B **71**, 214402 (2005).
[14] S. P. Singh, A. K. Singh, and D. Pandey, J. Phys.: Condens. Matter **19**, 036217 (2007).
[15] J. Rodriguez-Carvajal, FULLPROF, Laboratory Leon Brillouin (CEA-CNRS) CEA/Saclay, 91191 Gif sur Yvette Cedex, France, 2006.
[16] M. Jenhi, E. H. El Ghadraoui, H. Bali, M. El Aatmani, and M. Rafiq, Eur. J. Solid State Inorg. Chem. **35**, 221 (1998).
[17] G. Caglioti, A. Paeoletti, and F. P. Ricci, Nucl. Instrum. **3**, 223 (1958).
[18] Ragini, R. Ranjan, S. K. Mishra, and D. Pandey, J. Appl. Phys. **92**, 3266 (2002); A. M. Glazer, P. A. Thomas, K. Z. Baba-Kishi, G. K. H. Pang, and C. W. Tai, Phys. Rev. B **70**, 184123 (2004); A. K. Singh and D. Pandey, *ibid.* **67**, 064102 (2003).
[19] R. J. Hill and H. D. Flack, J. Appl. Crystallogr. **20**, 356 (1987).
[20] D. Vanderbilt and M. H. Cohen, Phys. Rev. B **63**, 094108 (2001).
[21] T. Watanabe and K. Kohn, Phase Transitions **15**, 57 (1989).
[22] D. Higashiyama, N. Kida, T. Arima, and Y. Tokura, Phys. Rev. B **70**, 174405 (2004).
[23] T. Kiyama, K. Yoshimura, K. Kosuge, Y. Ikeda, and Y. Bando, Phys. Rev. B **54**, 756 (1996).